Research Square

Preprints are preliminary reports that have not undergone peer review.
They should not be considered conclusive, used to inform clinical practice,
or referenced by the media as validated information.

Melatonin alleviates browning in fresh-cut Dioscorea hemsleyi in Weixi by enhancing antioxidant defense and modulating phenylpropanoid–flavonoid and sugar metabolism

Shihai Zhang
Southwest Forestry University
Lihong Zhao
Southwest Forestry University
Mei Zhang
Southwest Forestry University
Zhongjie Liu
Diqing Research Institute of Forestry and Grassland Science
Guijuan Zhao
Diqing Research Institute of Forestry and Grassland Science
Wenwu Yang
Southwest Forestry University
Xiaofei Feng
Southwest Forestry University
Xiangzhong Mao
Southwest Forestry University
Ning Zhao
Southwest Forestry University
Yun Liu
Southwest Forestry University
Dan Zong
skyzd907@swfu.edu.cn

Southwest Forestry University

Research Article

Keywords: Dioscorea hemsleyi in Weixi, Fresh-cut, Melatonin, Transcriptome, Metabolome

Posted Date: November 20th, 2026

DOI: https://doi.org/10.21203/rs.3.rs-11355960/v1

License: This work is licensed under a Creative Commons Attribution 4.0 International License.
Read Full License

Additional Declarations: No competing interests reported.

Melatonin alleviates browning in fresh-cut *Dioscorea hemsleyi* in Weixi by enhancing antioxidant defense and modulating phenylpropanoid–flavonoid and sugar metabolism

Shihai Zhang[1, 2] †, Lihong Zhao[1, 2] †, Mei Zhang[1, 2], Zhongjie Liu[3], Guijuan Zhao[3], Wenwu Yang[2], Xiaofei Feng[2], Xiangzhong Mao[2], Ning Zhao[2], Yun Liu[2*], Dan Zong[1, 2*]

† These authors contributed equally to this work

[1] Forest Resources Exploitation and Utilization Engineering Research Center for Grand Health of Yunnan Provincial Universities, Southwest Forestry University, Kunming 650224, China

[2] College of Biological Science and Food Engineering, Southwest Forestry University, Kunming 650224, China

[3] Diqing Research Institute of Forestry and Grassland Science, Diqing 674499, China

Corresponding author

liuyun@swfu.edu.cn (Y. Liu), skyzd907@swfu.edu.cn (D. Zong)

Abstract

Dioscorea hemsleyi in Weixi is an elite genetic resource and recognized geographical indication product, esteemed for its glutinous texture and nutritional benefits. Browning in fresh-cut yams reduces both quality and market value. Melatonin (MT) may alleviate this problem, but its exact mechanism of action in fresh produce is unknown. This study investigated the preventive effect of MT treatment on browning of fresh-cut *D. hemsleyi* in Weixi. The results showed that MT treatment significantly reduced the degree of browning of fresh-cut yam within four days of storage. Specifically, MT lowered the activities of polyphenol oxidase (PPO), peroxidase (POD), and phenylalanine ammonia-lyase (PAL), while it enhanced the activities of superoxide dismutase (SOD) and catalase (CAT). Furthermore, it decreased levels of hydrogen peroxide (H_2O_2) and superoxide (O_2^-), suppressed lipoxygenase (LOX) activity, and reduced malondialdehyde (MDA) accumulation. These actions resulted in decreased oxidative stress and diminished lipid peroxidation of membranes. In the metabolism related to phenylpropanoids and flavonoids, MT was found to downregulate essential biosynthetic genes (*PAL, 4CL, COMT, CAD, POD, CHS, CHI, C3'H, DFR, HTC*), as well as reduce the levels of downstream phenolic and flavonoid metabolites. MT also modulates the expression of several genes associated with starch and sucrose metabolism, including *SUS, AMY, INV*, and *TPP.* This regulation enhances the accumulation of soluble sugars, such as glucose, fructose, and sucrose, while simultaneously reducing the level of glucose-6-phosphate. In summary, these results suggest that MT slows down browning by direct suppression of browning-related enzymes, improved antioxidant capacity, and regulation of phenylpropanoid–flavonoid metabolism. These changes help preserve yam

quality and delay deterioration during storage.

Keywords: *Dioscorea hemsleyi* in Weixi; Fresh-cut; Melatonin; Transcriptome; Metabolome

1. Introduction

Dioscorea hemsleyi, also referred to as sticky yam, is a twining herbaceous vine that falls within the apical-winged clade of the *Dioscorea* genus. This plant is noteworthy for its underground tubers, which are known to be rich in mucopolysaccharides, starch, and various other compounds. Traditionally, these tubers have been utilized in medicinal practices, recognized for their beneficial effects on invigorating the spleen, eliminating excess moisture from the body, and tonifying both the lungs and kidneys [1, 2]. *D. hemsleyi* in Weixi is a unique yam germplasm endemic to Weixi County, Yunnan Province, and its adjacent high-altitude regions. Although it belongs to the same genus as *D. polystachya,* it is an independent species [3]. Adapted to high-altitude plateau environments at 2,000–3,000 m, it has tubers that are tender and glutinous, rich in nutrients and bioactive compounds, and exhibit distinctive quality traits [4]. In the past ten years, the global fresh fruit and vegetable market is also growing, ropelled by an increasing consumer inclination towards items that are fresh, convenient, free from additives, and nutritionally beneficial [5, 6]. While fresh-cut yams, such as *D. hemsleyi*, are recognized for preserving a rich array of nutrients, they are especially prone to mechanical harm during the processing phase. Such damage poses a threat to cellular compartmentalization, which can lead to an undesirable reaction in which enzymes associated with browning interact with their phenolic substrates. This interaction initiates a process of enzymatic browning that accelerates the deterioration of quality, consequently diminishing the commercial value of the produce [7, 8].

The color change observed in freshly cut yams is primarily attributed to enzymatic browning, a phenomenon resulting from the oxidation of polyphenolic compounds. This process is facilitated by enzymes such as polyphenol oxidase (PPO) and phenol peroxidase (POD) [9, 10]. Mechanical wounding of tissues triggers PPO and POD to catalyze polyphenol oxidation, producing α-quinone intermediates which subsequently polymerize to form brown complexes [11-13]. Therefore, effective inhibition of browning in fresh-cut yams generally requires regulating the generation of phenolic precursor compounds and interrupting the subsequent oxidative reactions. Various approaches have been explored for controlling browning of fresh-cut yam, including composite coatings incorporated with star anise essential oil [14], ethanol immersion [15], ascorbic acid dipping [16], sodium citrate soaking [17], combined ethanol–ascorbic acid treatment [18], oxalic acid treatment [8], and high-temperature curing [19]. Nonetheless, each of these methods has significant drawbacks. it is imperative to develop safe and economical approaches for prolonging the shelf life of fresh-cut yam while preserving its commercial value.

Melatonin (MT) is a ubiquitous indoleamine hormone in plants, including apples, tomatoes, cherries, cucumbers, berries, and peppers [20, 21]. It serves as a crucial regulator of key physiological processes in plants, including growth, senescence, and environmental stress tolerance [22]. Melatonin is a powerful antioxidant, which helps in maintaining the structural integrity of plant cells. It achieves this by addressing DNA damage and decreasing the

accumulation of harmful peroxides through the scavenging of free radicals [23]. Additionally, it enhances the plant's antioxidant defenses and reduces lipid peroxidation, crucial for keeping plant cells healthy and functional. Due to these advantageous properties, melatonin is often used to preserve fruits and vegetables after harvestt [24]. The hormone has proven effective in preventing the browning of plant tissues during culture by suppressing the oxidation of phenolic compounds, which are responsible for discoloration [25]. Research indicates that the application of melatonin in broccoli significantly prolongs its freshness and quality by delaying the onset of yellowing and the natural aging process known as senescence [26]. Furthermore, reports have demonstrated that exogenous melatonin effectively delays senescence and decay in sweet cherries [27], while also alleviating browning and preserving the nutritional quality of fresh-cut pears [28]. These collective findings indicate that melatonin holds significant promise for alleviating browning issues in fresh-cut horticultural products. However, despite the apparent benefits, the specific mechanisms by which melatonin exhibits its browning-inhibitory effects when used alone, particularly in the context of fresh-cut *D. hemsleyi* in Weixi, are not yet thoroughly understood. This gap in knowledge significantly impedes the specific use of melatonin for preserving yam products, indicating that additional research is necessary to fully explore its capabilities.

The present study aimed to investigate the impacts of melatonin treatment on the physiological, biochemical, and quality attributes of fresh-cut *D. hemsleyi* in Weixi. Uniform pieces of fresh yam were cut, soak in a MT solution for 30 minutes, and then kept at 25℃ for a duration of 4 days. Transcriptomic and metabolomic analyses were employed in this study to evaluate variations in gene expression profiles and metabolite contents between fresh-cut yam samples treated with MT and their untreated counterparts. An integrated multi-omics strategy was then adopted to elucidate the molecular mechanisms underlying MT-mediated browning inhibition and shelf-life extension of fresh-cut yam. The present study seeks to provide a scientific basis for the application of MT as a cost-effective preservation strategy for postharvest *D. hemsleyi* in Weixi and other tuber crops.

2. Materials and methods

2.1. Sampling and preparation of *D. hemsleyi* in Weixi

In December 2025, *D. hemsleyi* tubers were purchased from local farmers in Lari Village, Baohe Town, Weixi County, Yunnan Province, China (27.16°N, 99.30°E; 2350 m). The samples were transported to the laboratory within 24 hours. Healthy and uniform tubers, weighing between 500 and 800 grams, measuring 70 to 90 centimeters in length, and with diameters ranging from 3 to 5 centimeters, were selected for further experimentation. All tuber samples were preconditioned at 4 °C and 80-85% relative humidity for 24 hours before subsequent processing.

To examine how different concentrations of MT impact the inhibition of browning, slices of *D. hemsleyi* in Weixi were thoroughly cleaned, deprived, and cut into pieces measuring

approximately 5 ± 1 mm in thickness. Yam tablets were then immersed in melatonin solutions at concentrations of 0, 1, 2, 3, and 4 mmol/L for 30 min, and subsequently kept at room temperature for an additional 30 min to drain off surface moisture. Treatment with 0 mmol/L melatonin was used as the control group (CK). Ultimately, all yam slices were hermetically sealed in polyethylene film bags (0.02 mm thick) and stored at 25℃ with a relative humidity of 65 ± 2%. Browning-related indexes were measured daily over the entire storage period.

To evaluate the anti-browning effect of 3 mmol/L MT treatment, identical treatment protocols and storage conditions as described above were applied. The sole alteration was in the quantity of yam slices allocated to each group. In this study, every group consisted of 180 slices, organize this into three independent group, each containing 60 slices. Color changes of three yam tablets from each replicate were monitored continuously throughout the storage period. The remaining yam slices were set aside for subsequent sampling. At each sampling time point, two yam tablets were randomly picked from each biological replicate. Slices from the same replicate were diced into small pieces, homogenized thoroughly, and pooled into one composite sample (termed a biological replicate) to minimize variability among individual slices. Throughout storage, three biological replicates were sampled daily (on days 0, 1, 2, 3, and 4) for subsequent biochemical analysis. Harvested samples were snap-frozen in liquid nitrogen and kept at − 80℃ for downstream transcriptomic and large-scale metabolomic analyses.

2.2. Determination of cut-surface color and weight loss in fresh-cut *D. hemsleyi* in Weixi

The values for L^*, a^*, and b^* of yam slices were obtained using an automatic color-difference meter (3nh NS810, China). Browning was evaluated following the method of Min et al. [29], by measuring the absorbance at 410 nm and multiplying the value by 10. Weight loss of fresh-cut yam was determined using the gravimetric method described by Wu et al. [30].

2.3. Analysis of enzymatic browning-related parameters

2.3.1.Determination of browning-associated enzyme activities

The evaluation of PPO and POD activities was conducted based on the methods outlined by Mishra et al. [31] and Chen et al. [32], incorporating slight adjustments. To summarize, a 0.1 g sample of frozen yam tissue was pulverized and mixed in an ice bath with 0.5 mL of the extraction solution. The phosphate buffer at pH 6.0 was used for the PPO analysis, while for POD, PBS at pH 7.8 was utilized. The resulting homogenate underwent centrifugation at 10,000 × *g* for 10 minutes at 4℃, after which the supernatant was extracted for enzyme assays. In conducting the PPO assay, the enzyme extract was combined with 0.1 mL of catechol solution in the phosphate buffer at pH 6.0. Following a 15-minute incubation at 37℃, the reaction was halted by placing the mixture on ice for 3 minutes, and it was then centrifuged at 10,000 × *g* for an additional 10 minutes. The absorbance of the resulting supernatant was recorded at 410 nm. For the POD assay, 57 μL of the supernatant was mixed with 157 μL of a working reagent, composed of 100 mM phosphate buffer (pH 6.0), guaiacol,

and H_2O_2 in the preparation ratios of 104:26:27. Absorbance changes at 470 nm (ΔA) were monitored from 30 to 90 s after mixing. For both PPO and POD, one unit of activity was defined as a 0.01 absorbance change per minute per gram of fresh weight, and enzyme activity was expressed as $U \cdot g^{-1} \cdot min^{-1}$.

PAL activity was assayed according to the method of Wei et al. [33], with minor modifications. Tissue powder (0.1 g) was homogenized in 0.5 mL extraction buffer composed of 100 mM sodium borate buffer (pH 8.8) containing PVP, EDTA, and β-mercaptoethanol. The mixture was then centrifuged at 10,000 × *g* for 10 min at 4℃. The reaction system consisted of 8 μL supernatant, 312 μL 50 mM borate buffer (pH 8.8), and 80 μL 20 mM L-phenylalanine. After incubation at 30℃ for 30 min, the reaction was stopped by adding 16 μL 6 M HCl. Following 10 min equilibration, absorbance was read at 290 nm against a blank. PAL activity was calculated from the absorbance change of 0.1 min^{-1} g^{-1} tissue, and results were expressed as $U \cdot g^{-1} \cdot min^{-1}$.

2.3.2. Measurement of H_2O_2, O_2^-, and MDA levels and activities of SOD, CAT, and LOX

Hydrogen peroxide (H_2O_2), superoxide anion O_2^-, and malondialdehyde MDA contents, together with superoxide dismutase SOD, catalase CAT, and lipoxygenase LOX activities, were measured using commercial assay kits from Solarbio (Beijing, China) following the manufacturer's instructions. H_2O_2 and O_2^- levels were expressed as μmol g^{-1} FW, MDA content as nmol g^{-1} FW, and enzyme activities as U mg^{-1} protein.

2.3.3. Determination of total phenolics and flavonoids

Total phenolics and flavonoids were quantified by the Folin-Ciocalteu and aluminum nitrate colorimetric assays, respectively, using gallic acid and rutin as standards [34, 35]. In brief, yam powder (0.1 g) was extracted with 0.5 mL of 60% ethanol at 60℃ for 30 min under ultrasonication, then centrifuged at 10,000 × *g* for 10 min at 25℃. For total phenolics, the supernatant was reacted with Folin-Ciocalteu reagent and Na_2CO_3, and absorbance was read at 760 nm. In contrast, flavonoid contents were measured at 510 nm after the supernatant's reaction with $NaNO_2$, $Al(NO_3)_3$, and NaOH. The results were derived from standard curves and reported as mg/g.

2.4. Transcriptomic and metabolomic analyses

Transcriptomic and metabolomic datasets were compared across two groups of fresh-cut *D. hemsleyi* in Weixi: control slices at day 0 and after 3 days of storage (CK0d and CK3d), and MT-treated slices at day 0 and after 3 days of storage (MT0d and MT3d). Each treatment comprised three biological replicates for transcriptomic and metabolomic profiling.

2.4.1. Transcriptomic analysis

Total RNA was isolated from frozen yam tissues with a commercial RNA extraction kit (DP441, Tiangen, China) according to the manufacturer’s instructions. RNA integrity and quality were assessed using a NanoDrop spectrophotometer and an Agilent 2100 Bioanalyzer, with an RIN cutoff of ≥ 7.0. Sequencing libraries were constructed with the Hieff NGS® Ultima Dual-mode mRNA Library Prep Kit following the standard workflow: poly(A)

enrichment, fragmentation, cDNA synthesis, adapter ligation, and magnetic bead purification. Libraries passing quality control were sequenced on an Illumina NovaSeq 6000 platform with paired-end 150 bp (PE150) sequencing. Raw read sequences 206 underwent trimming with Trimmomatic (v0.39). De novo assembly of cleaned reads into unigenes was performed using Trinity. Gene expression quantification was conducted based on FPKM, achieved by re-aligning the reads to the assembled unigenes with Bowtie2 and RSEM. The detection of differentially expressed genes (DEGs) utilized DESeq2, applying criteria of $|\log_2(\text{fold change})| \geq 1.0$ and an adjusted p - value of less than 0.01. The functional annotation of the unigenes was accomplished through BLAST searches against the NR, GO, and KEGG databases.

2.4.2. Metabolomic analysis

Widely targeted metabolomics was applied to profile yam slice metabolites and to assess MT-induced changes. Yam tissue (50 mg), after grinding in liquid nitrogen, was extracted using 1 mL of a methanol–acetonitrile–water (2:2:1) mixture containing 20 μg/mL isotope-labeled internal standards. The mixture was vortexed, kept on ice for 5 min, and then centrifuged (12,000 × *g*, 10 min, 4℃). The supernatant was harvested and adjusted to 53% methanol with LC-MS grade water, followed by another centrifugation under identical conditions. The supernatant was analyzed by UPLC-QTOF-MS/MS using a Waters Acquity I-Class PLUS/Xevo G2-XS system equipped with an HSS T3 column (2.1 × 100 mm, 1.8 μm). The mobile phase consisted of 0.1% formic acid in water (A) and 0.1% formic acid in acetonitrile (B), with a gradient program optimized for polar metabolites. MS data were acquired in both positive and negative ionization modes.

The processing of raw data was conducted with Progenesis QI and XCMS software. Identification of metabolites involved comparing the MS/MS spectra to an in-house database, utilizing retention time, precursor ion (Q1), and product ion (Q3) details. Differentially abundant metabolites (DAMs) were selected according to the following criteria: $|\text{fold change}| \geq 1.5$, adjusted $p < 0.05$, and VIP > 1, as determined by orthogonal partial least-squares discriminant analysis (OPLS-DA). Functional annotation and pathway enrichment analyses of DAMs were performed using the KEGG database.

2.5. RT-qPCR analysis

Total RNA was isolated with TRIzol reagent, and first-strand cDNA was synthesized using the Hifair® III 1st-strand cDNA Synthesis SuperMix for qPCR (Shanghai Yeasen Biotechnology Co., Ltd., China). The Protein Phosphatase 2 (PP2A) gene was selected as the endogenous reference for normalizing gene expression, and relative expression was computed using the $2^{-\Delta\Delta Ct}$ approach [36]. Primer Premier 5.0 was employed to design primers covering exon–exon junctions for specific amplification (Table S1).

2.6. Statistical analysis

Statistical analyses were conducted using IBM SPSS Statistics 21.0. Differences between control and MT-treated groups were evaluated by Student's t-test, with $P < 0.05$ considered

statistically significant. Significance levels are indicated by asterisks (*) in the figures. Data are expressed as mean ± standard deviation (SD) of three independent replicates (n = 3).

3. Results

3.1. Screening of optimal MT concentration and its browning inhibition efficacy

The present study was designed to determine the optimal melatonin (MT) concentration for browning inhibition in fresh-cut yam slices. To achieve this, we evaluated the browning-inhibitory effects of several MT concentrations, specifically 1, 2, 3, and 4 mmol/L. The results revealed that the CK group exhibited a sharp decline in L^* values, accompanied by significant increases in both a^* and b^* values, along with a greater overall browning extent. These results demonstrated that browning on the surface of fresh-cut yam progressively increased during storage (Figure S1). By contrast, MT-treated groups at different concentrations showed markedly smaller changes in browning-associated parameters during the 4-day storage period. The findings suggest that MT successfully inhibited browning in fresh-cut yam slices, supported 256 by the data shown in Figure S1A – E. When comparing the browning degrees on day four, the yam slices treated with 1, 2, 3, and 4 mmol/L of MT exhibited reductions in browning of 16.17%, 44.26%, 47.84%, and 39.76%, respectively, relative to the CK group (Figure S1D). Overall, despite all tested MT concentrations reducing browning of fresh-cut yam, the 3 mmol/L MT treatment exhibited the greatest inhibitory effect. Consequently, this concentration was selected as the optimal one for further experiments, given its superior capability in minimizing browning.

3.2. MT treatment inhibits browning of fresh-cut of *D. hemsleyi* in Weixi

To further assess the effectiveness of MT in inhibiting browning, a series of repeated validation experiments was conducted using the optimal concentration of 3 mmol/L MT. The results from these experiments clearly demonstrated that the use of MT considerably decreased the incidence of surface browning in fresh-cut yam when compared with the CK group (Fig. 1A). yam compared with the CK group (Fig. 1A). Despite a progressive rise in browning of fresh-cut yam across both MT and CK groups throughout storage, MT-treated yams maintained a markedly lower browning degree. Quantitatively, the CK group exhibited 1.92-fold greater browning than the MT-treated group (Fig. 1B).

Color parameters L^*, a^*, and b^* of fresh-cut yam slices were measured, and ΔE was computed to quantify the degree of visual browning. In comparison with the CK group, MT treatment markedly attenuated both the decrease in L^* and the increase in a^* and b^* of fresh-cut yam slices (Fig. 1C–E). During storage, ΔE values for the MT treatment remained consistently lower than those documented for the CK (Fig. 1F). Collectively, these results indicate that MT treatment effectively retards browning of fresh-cut yam. Furthermore, with prolonged storage, the weight loss rate of the MT-treated group was markedly lower than that of the CK group. On day 4, the MT group showed a weight loss rate 1.5% below that of the CK group (Fig. 1G).

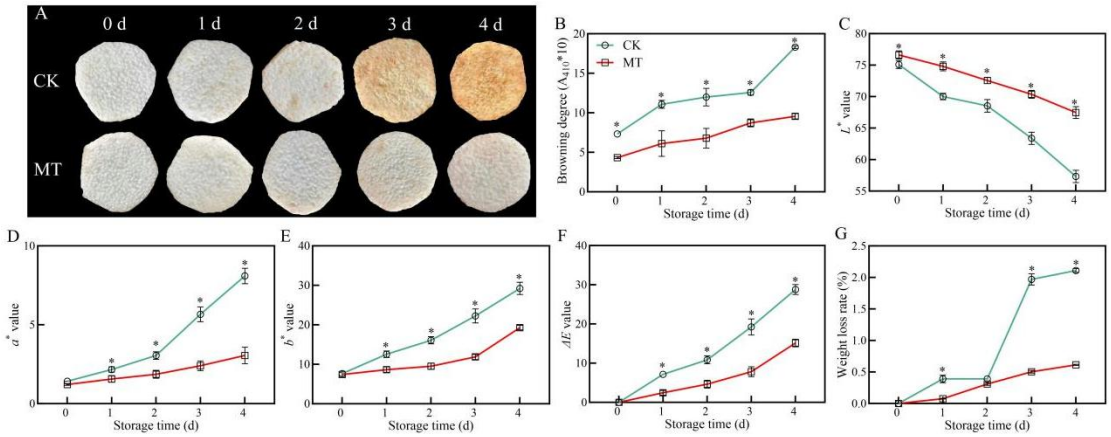


Fig. 1 Trends in color parameters of *D. hemsleyi* in Weixi under different storage durations. **A** Browning appearance of representative Weixi glutinous yam slices following 4 d of storage at 25 ℃. External appearance, **B** browning degree, **C** *L**, **D** *a**, **E** *b**, and **F** *ΔE* value of fresh-cut Weixi glutinous yam. **G** Weight loss. Asterisks indicate statistically significant differences ($P < 0.05$) among treatment groups at each time point, as assessed by Student's t-test.

3.3. Effects of MT on the physiological and biochemical properties of *D. hemsleyi* in Weixi

3.3.1. Enzyme activities related to browning

During the assessment of shelf life over a period of four days, notable differences were observed in the dynamic changes of polyphenol oxidase (PPO), peroxidase (POD), and phenylalanine ammonia-lyase (PAL) activities between the MT treatment group and the CK group. In the MT treatment group, PPO activity showed a gradual decline between day 1 and day 3 and a subsequent rise on day 4, while the CK group displayed a continuous increase throughout the whole period (Fig. 2A). Significant differences emerged only on day 0; from day 1 to day 4, the results remained consistent (Fig. 2A). POD activity increased in all samples, but the rise in the MT group was gradual and even showed a subsequent decline. Overall, POD activity in the MT-treated group was consistently and markedly lower than that in the CK group (Fig. 2B). Additionally, PAL activity displayed a varying pattern, with an overall upward trend across all treatments: the CK group increased steadily over time, while the MT group first decreased during the initial two days and then experienced a sharp rise in the following two days, reaching its peak on day 4. Nevertheless, throughout the entire experimental period, PAL activity in MT-treated samples remained markedly lower than that in the CK group (Fig. 2C).

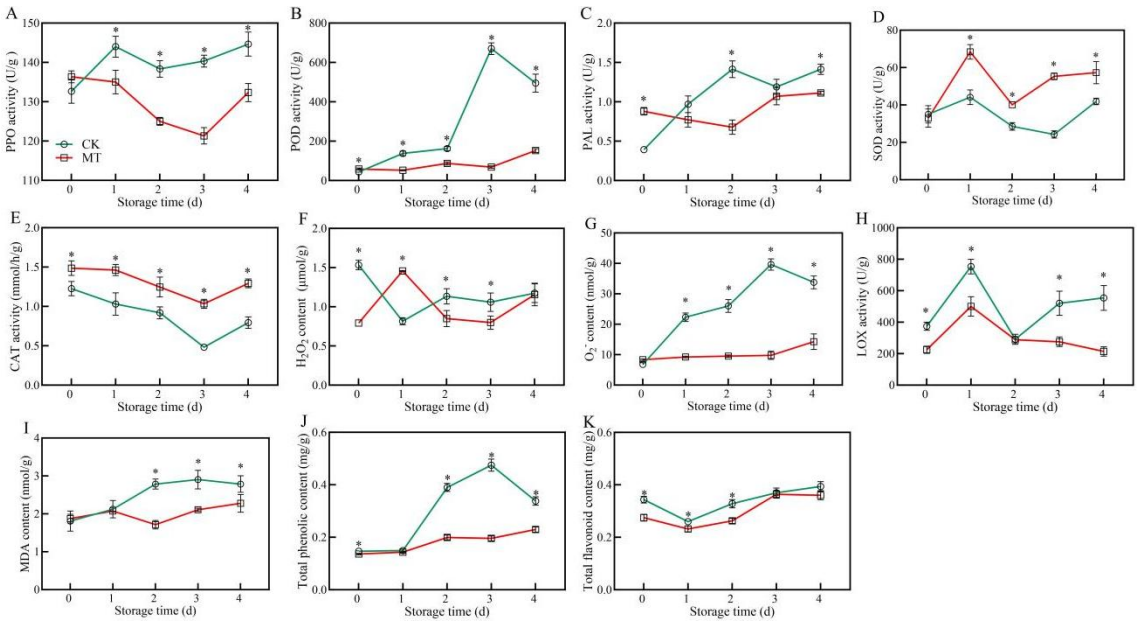


Fig. 2 Physiological and biochemical changes in fresh-cut *D. hemsleyi* in Weixi in response to MT treatment, compared with the CK during storage. **A** PPO activity. **B** POD activity. **C** PAL activity. **D** SOD activity. **E** CAT activity. **F** H_2O_2 content. **G** O_2^- content. **H** LOX activity. **I** MDA content. **J** Total phenolic content. **K** Total flavonoid content. Values are expressed as mean ± SD (n = 3). Asterisks indicate significant differences ($P < 0.05$) between treatment groups at each sampling time, as determined by Student's t-test.

3.3.2 Reactive oxygen metabolism and oxidative stress after MT treatment

Superoxide dismutase (SOD) activity in both groups showed an initial rise, then decreased and subsequently increased. Notably, MT-treated samples showed consistently and significantly higher SOD activity than the CK group (Fig. 2D). Likewise, catalase (CAT) activity exhibited a comparable trend in both groups, with MT-treated samples exhibiting significantly higher activity throughout storage (Fig. 2E). In the control group, hydrogen peroxide (H_2O_2) levels dropped on day 1, before progressively increasing thereafter. Conversely, the MT-treated group experienced fluctuations, reaching a peak on day 1 but sustaining significantly lower H_2O_2 levels compared to the CK group until day 4, when the differences were no longer significant (Fig. 2F). In the CK group, superoxide anion (O_2^-) levels rose steadily during storage, while MT groups showed a more gradual increase (Fig. 2G). Generally, MT groups had significantly lower O_2^- concentrations than the CK group, with the exception of day 0. After 4 days of storage, the MT group exhibited a 57.76% reduction in O_2^- levels compared with the CK group. This indicates that melatonin treatment markedly reduced O_2^- content in fresh-cut yam.

3.3.3. Effects of MT treatment on lipid peroxidation of *D. hemsleyi* in Weixi

The effect of MT treatment on lipid peroxidation was further assessed by monitoring lipoxygenase (LOX) activity and malondialdehyde (MDA) accumulation (Fig. 2H and 2I). Both groups exhibited similar trends in LOX activity; however, the MT group consistently showed a significantly reduced activity throughout the storage duration. Notably, the MT

group exhibited a 61.33% decrease in LOX activity compared with the CK group, indicating that MT treatment effectively inhibits LOX activity in fresh-cut yam. Conversely, the MDA levels in the CK group rose continuously, whereas the increase in MDA levels in the MT group was more gradual, reaching its lowest point on day 2 and remaining consistently below those observed in the CK group. On day 4, MDA levels in the MT-treated group were 18.71% lower than those in the CK group, supporting the view that melatonin treatment effectively retards MDA accumulation in fresh-cut yam.

3.3.4. MT treatment effects on total phenolic and flavonoid contents of *D. hemsleyi* in Weixi

Over the 4-day storage period, both groups showed a gradual increase in total phenolic and flavonoid contents. Nevertheless, MT-treated samples maintained markedly lower levels than the CK group (Fig. 2J and 2K). This difference became especially evident after 2 days, at which point total phenolic content in the CK group was double that in the MT group. In contrast, flavonoid content did not differ significantly after 2 days.

3.4. Transcriptomic and metabolomic analyses

3.4.1. Transcriptome analysis

Heatmaps from PCA and Pearson correlation of transcriptome datasets for *D. hemsleyi* in Weixi slices—obtained from CK and MT treatments and freshly prepared at 0 and 3 days of storage—verified data reliability within the same sample group and revealed statistically significant differences among distinct groups (Fig. 3A and 3B). Comparative transcriptomics revealed a total of 1,327 differentially expressed genes (DEGs) when comparing CK0d with MT0d (including 664 upregulated and 663 downregulated genes) and identified 4,467 DEGs in the CK3d versus MT3d comparison (with 2,480 upregulated and 1,987 downregulated genes), of which 371 DEGs were shared between the two comparisons (Fig. 3C and 3D). The DEGs identified in the CK3d versus MT3d analysis may correlate with the differences observed in browning and were chosen for subsequent analysis. The most significantly enriched GO functional categories for DEGs in the CK3d versus MT3d comparison included carbohydrate metabolism, oxidoreductase activity, and microtubule binding (Fig. 3E). The leading 20 enriched KEGG pathways identified for the DEGs in the CK3d 360 compared to the MT3d analysis included flavonoid biosynthesis, metabolism of starch and sucrose, as well as phenylpropanoid biosynthesis and tyrosine metabolism, among other pathways (Fig. 3F).

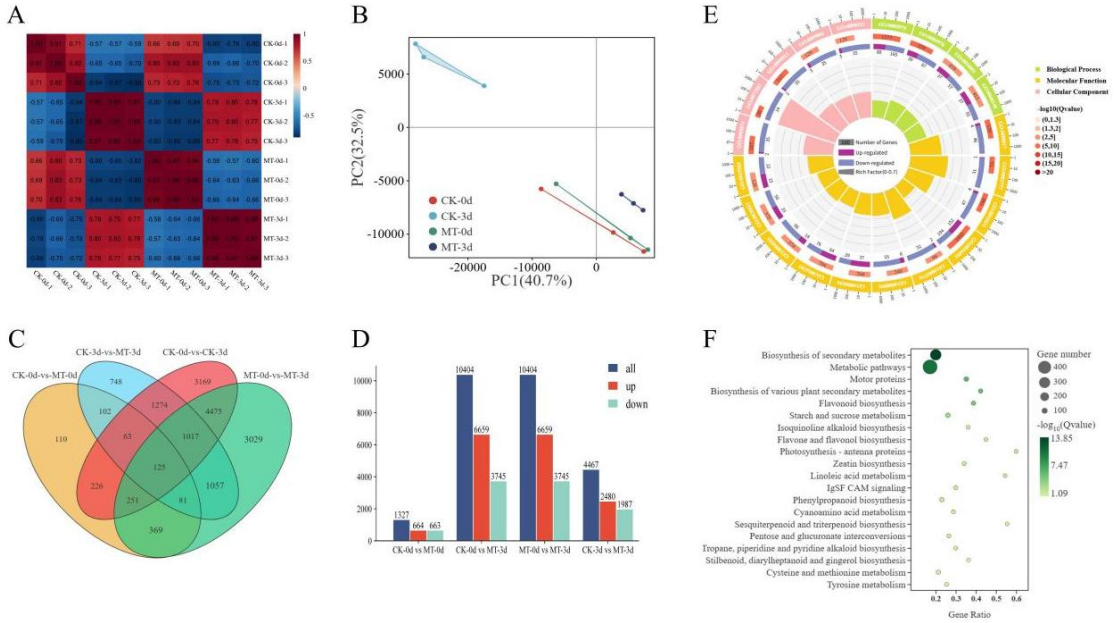


Fig. 3 Transcriptome analysis of *D. hemsleyi* in Weixi was performed for both CK and MT groups at different storage time points. **A** A heatmap illustrating Pearson correlation coefficients that depict gene expression in yam specimens across distinct treatment conditions. **B** PCA plot presenting transcriptome profiles of yam samples across various treatments. **C** Venn diagrams illustrating differential gene sets from yam specimens in contrasting treatment group comparisons. **D** Bar chart showing the number of DEGs in different treatment comparisons. **E** A comparison of DEGs between CK-3d and MT-3d treatment groups enriched in the Gene Ontology (GO) database, highlighting the lowest significant p-value. From the outer to the inner layers: the first arc details the ID of the GO term; the second arc's hue indicates the p-value, while its length illustrates the total gene count found in this category, referred to as background genes; the third arc displays the number of DEGs associated with this term; and the fourth arc signifies the enrichment factor. **F** Bubble charts showing DEGs among the top 20 pathways with the smallest p-value based on the KEGG database for the CK-3d vs. MT-3d comparison..

3.4.2. Metabolomic analyses

The validity of the model was strongly supported by Pearson correlation and OPLS-DA, demonstrating R^2Y values approaching 1 and Q^2Y exceeding 0.5, which indicates significant metabolic differences between the CK and MT treatment groups (Fig. 4A and 4B). A comparative examination identified 98 distinctively abundant metabolites (DAMs) in the comparison between CK0d and MT0d, as well as 153 DAMs in the CK3d versus MT3d analysis (Fig. 4C). The volcano plot illustrated that in the CK3d vs. MT3d comparison, 67 metabolites exhibited increased levels, while 86 showed decreased levels (Fig. 4D). KEGG enrichment analysis revealed that pathways related to secondary metabolite biosynthesis showed the strongest enrichment of DAMs in CK3d compared with MT3d. The 20 most enriched pathways comprised starch and sucrose metabolism, flavonoid biosynthesis, isoflavonoid biosynthesis, and phenylpropanoid biosynthesis (Fig. 4E). A combined analysis of co-enriched DEGs and DAMs (CK3d vs. MT3d) revealed specific metabolic processes showing differential regulation across treatment groups. This further supports the notion that

MT treatment has a selective impact on the networks involved in flavonoid biosynthesis (Fig. 4F).

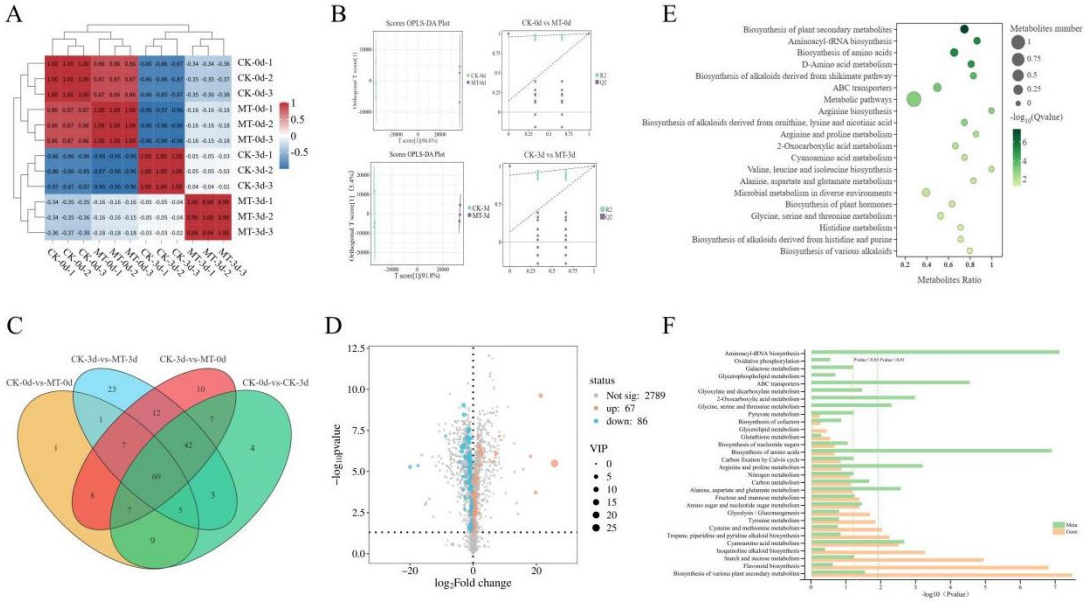


Fig. 4 Metabolomic profiles of fresh-cut *D. hemsleyi* in Weixi tissues were analyzed in both CK and MT groups at various storage time intervals. **A** A heatmap illustrating Pearson correlation of fresh-cut yam samples across various treatment groups. **B** Score plots obtained by OPLS-DA were used to compare yam samples between CK-0d and MT-0d, and between CK-3d and MT-3d. These are presented alongside the corresponding replacement test plots for their OPLS-DA models. A Q^2Y value that exceeds 0.5 suggests that the model is valid, whereas a Q^2Y exceeding 0.9 indicates an excellent model, which can be employed for the identification of differential metabolites through the analysis of variable importance projections. **C** Venn diagrams illustrating the groups of differentially abundant metabolites (DAMs) identified in yam samples across various treatment comparisons. **D** Volcano plots showcasing DAMs in yam samples comparing CK-3d versus MT-3d treatment groups. In the plot, blue points indicate DAMs with decreased abundance, while red points depict those with increased abundance, and gray points denote detected metabolites without significant differences in abundance. **E** Bubble plots illustrating DAMs within the top 20 enriched pathways that exhibit the lowest p-values of significance from the KEGG database for the CK-3d versus MT-3d treatment group comparison. **F** An integrated analysis of transcriptome and metabolome focusing on DAM enrichment among the top 30 pathway entries with the smallest significant p-value in the KEGG database concerning the CK-3d versus MT-3d treatment group comparison.

3.5. Phenylpropanoid metabolism

To examine the effect of MT treatment on gene and metabolite expression associated with phenylpropanoid metabolism in fresh-cut *D. hemsleyi* in Weixi, we analyzed DEGs and DAMs. Comparative transcriptome profiling of CK and MT groups at day 0 and day 3 identified 30 DEGs linked to 9 key enzymes involved in the phenylpropanoid biosynthesis pathway (ko00940) (Fig. 5A). Compared to CK levels, critical genes within the phenylpropanoid metabolism pathway exhibited down-regulation on days 0 and 3 in the MT

treatment group. The encoded enzymes include phenylalanine ammonia-lyase (*PAL*), 4-coumarate–CoA ligase (*4CL*), caffeic acid 3-O-methyltransferase (*COMT*), trans-cinnamate 4-monooxygenase (*CYP73A*), 5-O-(4-coumaroyl)-D-quinate 3'-monooxygenase (*C3'H*), coniferyl-aldehyde dehydrogenase (*REF1*), peroxidase (*E1.11.1.7, POD*), cinnamyl-alcohol dehydrogenase (*CAD*), and shikimate O-hydroxycinnamoyltransferase (*HTC*) (Fig. 5A and 5B). In the CK3d group, the levels of expression for *PAL, 4CL3, COMT, CAD,* and *POD3* were identified to be 3.58, 5.64, 3.40, 16.41, and 25.15 times higher in comparison to the MT3d treatment (Fig. 5C). RT-qPCR validation corroborated the trends seen in the corresponding FPKM values (Figure S2A–S2E). Moreover, these results aligned with PAL and POD enzyme activities, which were significantly lower in the MT group relative to the CK group (Fig. 2B and 2C). Furthermore, the abundance of downstream metabolites involved in phenylpropanoid metabolism was substantially greater in the MT3d group than in the CK3d group (Fig. 5D). This reduction in metabolic activity is in agreement with the expression trends of the majority of the DEGs linked to phenylpropanoid metabolism.

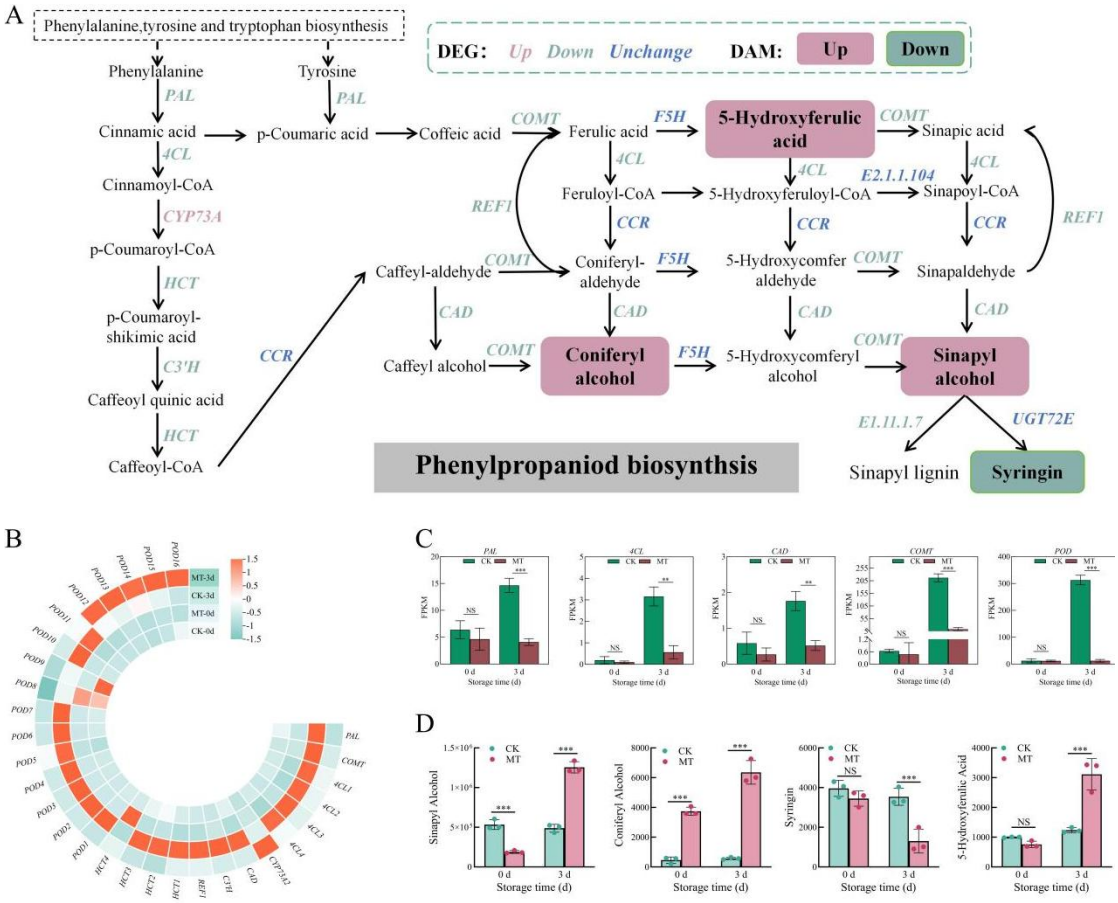


Fig. 5 Phenylpropanoid metabolism in fresh-cut *D. hemsleyi* in Weixi treated with CK and MT during storage. **A** Genes that are DEGs and metabolites that are DAMs associated with phenolic metabolism were examined in the comparison between CK and MT (MT-treated). **B** Heatmap displaying FPKM expression values of DEGs identified from pairwise comparisons (CK0d vs. MT0d and CK3d vs. MT3d), mapped onto the phenylalanine biosynthesis pathway. **C** Expression profiles of key DEGs from

the CK0d vs. MT0d and CK3d vs. MT3d comparisons are illustrated in the phenylpropanoid biosynthesis pathways. **D** Relative levels of DAMs identified from the same comparisons are also depicted in these pathways. Data are expressed as mean ± SD (n = 3). Asterisks (*) indicate significant differences ($P < 0.05$) between CK and MT groups, as determined by t-test.

3.6. Flavonoid-related metabolism

Transcriptome profiling revealed 26 differentially expressed genes (DEGs) that code for 10 crucial enzymes involved in three interconnected pathways of flavonoid biosynthesis: flavonoid (ko00941), isoflavonoid (ko00943), and the biosynthesis of flavones and flavonols (ko00944) during the comparisons between CK and MT atat day 0 and day 3 of storage (Fig. 6A). Significantly, MT treatment decreased the expression of multiple genes related to flavonoid metabolism (7 of 10), including those involved in chalcone metabolism (chalcone synthase, *CHS*; chalcone isomerase, *CHI*), anthocyanin modifiers (anthocyanidin reductase, *ANR*), and regulators of hydroxylation/redox processes (flavonoid 3′-monooxygenase, *CYP75B1*; bifunctional dihydroflavonol 4-reductase, *DFR*). Moreover, genes responsible for hydroxylation/redox regulation (chalcone 3-hydroxylase, *C3'H*) and anthocyanin-modifying enzymes (hydroxycinnamoyl-CoA: anthocyanin-3-glucoside-6"-O-hydroxycinnamoyltransferase, *HTC*) were also downregulated. In contrast, only the anthocyanin-modifying enzymes (UDP-glucose: anthocyanin 5-O-glucosyltransferase, *PGT*) and hydroxylation/redox regulatory genes (cytochrome, CYP73A2) were observed to be upregulated (Fig. 6A). In the MT treatment group, *CHS1, CHI, C3'H, DFR*, and *HTC* expression was significantly reduced compared to the CK group, showing downregulation of 9.11, 5.33, 15.48, 22.92, and 74.19 times by day 3 (Fig. 6B). Validation through RT-qPCR demonstrated consistent patterns of downregulation for *CHS1, CHI, C3'H, DFR*, and *HTC*, corroborating the FPKM data (Figure S2F–S2J). Likewise, our metabolomic analysis showed that MT treatment caused a decrease in flavonoid metabolite levels in yam during storage compared with the CK group (Fig. 6D). These findings indicate that MT application modulates gene expression and metabolite profiles related to flavonoid metabolism, which may contribute to a notable decrease in browning of fresh-cut yam slices. This metabolic inhibition aligns with the observed downregulation of biosynthetic genes (Fig. 6B and 6C).

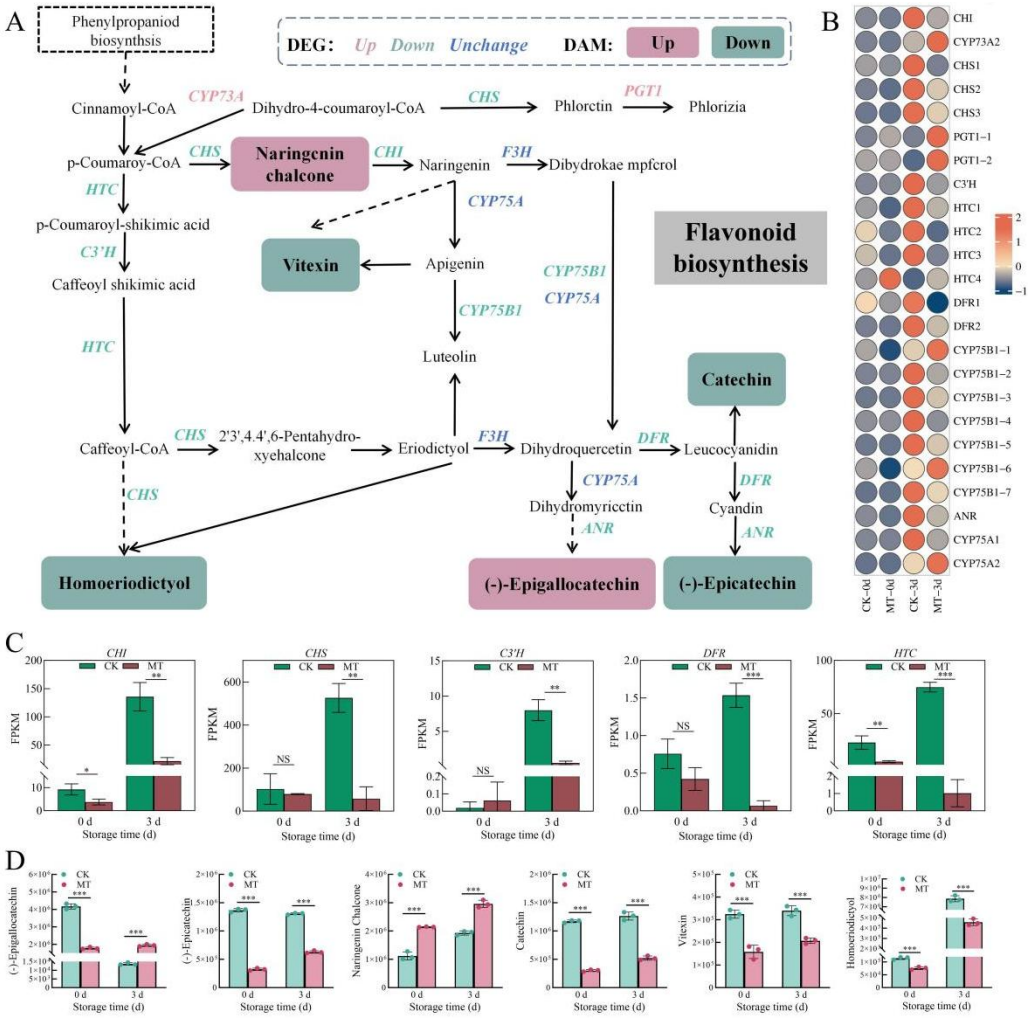


Fig. 6 Flavonoid metabolism, the biosynthesis of isoflavonoids, as well as the production of flavones and flavonols in fresh-cut *D. hemsleyi* in Weixi. subjected to CK and MT treatments during storage. **A** Genes that are DEGs and metabolites that are DAMs associated with flavonoid biosynthesis in the comparison between CK and MT (MT-treated). **B** Heatmap showing FPKM expression levels of DEGs identified from pairwise comparisons (CK0d vs. MT0d, CK3d vs. MT3d), assigned to the flavonoid biosynthesis pathway. **C** Expression patterns of key DEGs across the CK0d vs. MT0d and CK3d vs. MT3d comparisons are visualized in the flavonoid biosynthesis pathways. **D** Relative levels of DAMs identified from the CK0d vs. MT0d and CK3d vs. MT3d comparisons are projected onto the flavonoid biosynthesis pathways. Values are expressed as mean ± SD (n = 3). Asterisks (*) indicate significant differences ($P < 0.05$) between CK and MT groups, based on t-test.

3.7. Starch and sucrose metabolism

Comparison between CK3d and MT3d further investigated alterations in gene expression and metabolite profiles associated with starch and sucrose metabolism. Overall, 20 DEGs encoding 14 different proteins associated with this pathway were detected. Notably, genes encoding beta-glucosidase (*bglB*), beta-fructofuranosidase (*INV*), alpha-amylase (*AMY*), sucrose synthase (*SUS*), and trehalose-6-phosphate phosphatase (*TPP*) exhibited downregulated expression in MT3d compared with CK3d (Fig. 7A). Furthermore, the

majority of DEGs encoding carbohydrate metabolism enzymes—such as sucrose synthase (*SUS*), hexokinase (*HK*), trehalose-6-phosphate synthase (*TPS*), UDP-glucose pyrophosphorylase (*UGP*), ADP-glucose pyrophosphorylase large subunit (*APL*), glucose-6-phosphate isomerase (*GPI*), AMY, and sucrose-6-phosphate phosphatase (*SPP*)—showed upregulated expression in the MT3d group(Fig. 7B). The results from RT-qPCR for SUS and TPP corroborated the respective FPKM values across both sample groups (Figure S2K-S2O). In addition, downstream metabolites related to starch and sucrose metabolism—including D-glucose, sucrose, and D-fructose—were significantly higher in MT3d than in CK3d. By contrast, D-glucose 6-phosphate levels declined in the MT3d group during storage (Fig. 7C).

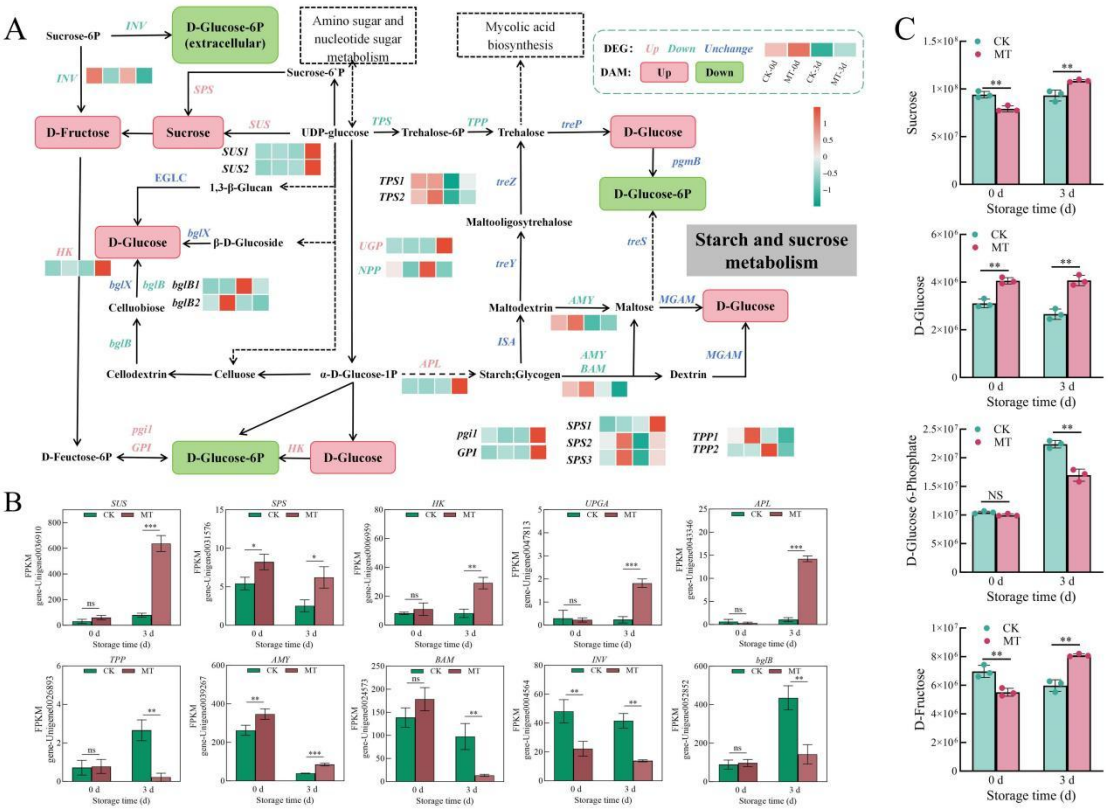


Fig. 7 Starch and sucrose metabolism in CK and MT-treated fresh-cut D. hemsleyi in Weixi during storage. **A** DEGs and DAMs identified from the CK0d vs. MT0d and CK3d vs. MT3d comparisons were assigned to the starch and sucrose metabolism pathway. Heatmaps represent FPKM values. **B** Expression patterns of key DEGs from the CK0d vs. MT0d and CK3d vs. MT3d comparisons are shown, annotated within the starch and sucrose metabolism pathway. **C** Relative levels of DAMs detected from the CK0d vs. MT0d and CK3d vs. MT3d comparisons were linked to the starch and sucrose metabolism pathway. Values are shown as mean ± SD (n = 3). Asterisks (*) denote significant differences ($P < 0.05$) between CK and MT groups, determined by t-test.

4. Discussion

D. hemsleyi in Weixi has a high moisture content and is nutrient-rich. Nevertheless, its active metabolism renders it susceptible to water loss, leading to wilting, browning, and ultimately spoilage during storage. Melatonin (MT) serves as a potent preservative, though its capacity to prevent browning is not as well acknowledged as that of conventional antioxidants. Research indicates that MT can effectively reduce browning in a variety of horticultural crops [37], yet its molecular mechanism remains ambiguous. In this study, we demonstrate that soaking in MT markedly reduces browning in fresh-sliced yam. Utilizing a multi-omics strategy, we further explored the mechanisms underlying MT-mediated metabolic reprogramming and showed that this strategy simultaneously modulates several signaling pathways to suppress browning and preserve quality.

Browning limits the marketability and shelf life of minimally processed vegetables, and its severity is commonly assessed by the degree of browning. During the browning process, L^* values decrease, while a^* and b^* values rise, providing a collective measurement of browning severity. In this research, treatment with MT resulted in enhanced visual quality, a reduced degree of browning, and minimized weight loss throughout the storage duration. This improvement was likely due to a reduction in enzymatic browning and a slowdown in postharvest senescence. The present findings align with those reported by Gao et al. [38], who demonstrated that melatonin alleviated browning severity and weight loss, attenuated the decrease in L^*, and inhibited the increase in a^*/b^* ratios of peach fruit. Comparable anti-browning effects have also been reported in fresh-cut lotus root [39] and potatoes[40].

Enzymatic browning of fresh-cut yam is mainly caused by PPO and POD [41]. PPO mediates the oxidation of endogenous phenolics into o-quinones, while POD employs H_2O_2 as a co-substrate for the oxidation of these phenolics, leading to pigment production [42]. Therefore, inhibiting PPO and POD activities is considered an effective strategy to reduce browning. In this study, we found that PPO and POD activities remained high in CK samples during storage, indicating their involvement in phenolic oxidation and subsequent browning. By contrast, PPO and POD activities in MT-treated samples decreased significantly, which was accompanied by reduced browning. Our findings align with previous reports on apple, where nicotinamide decreased POD and PPO activities and effectively inhibited browning of fresh-cut apple [43]. Similarly, another study showed that glutamic acid treatment markedly reduced both PPO and POD activities in fresh potatoes, thus inhibiting browning [44].Taken together, our physiological and multi-omics data support the notion that enzymatic browning is the main cause of browning in fresh-cut yam. MT treatment alleviates browning by suppressing the activities of enzymes implicated in enzymatic browning, such as PPO and POD. This conclusion is supported by the decreased enzyme activity and downregulated browning-related genes.

Cutting can cause mechanical damage that leads to the generation of significant quantities of ROS, such as O_2^- and H_2O_2. Overaccumulation of ROS exacerbates lipid peroxidation of membranes and compromises membrane integrity, thus promoting the onset

of enzymatic reactions [45]. Fresh-cut yam exhibits accelerated membrane lipid peroxidation and browning. Antioxidant enzymes such as CAT and SOD function as a key cellular defense system to combat oxidative stress by scavenging ROS and alleviating stress-induced cellular damage [46]. Studies have shown that MT-treated broccoli markedly increases SOD and CAT activities while concurrently reducing H_2O_2, O_2^-, and MDA levels [47]. Consistent with these findings, the present study demonstrates that MT treatment increases CAT and SOD activities in fresh-cut yam tissues while reducing H_2O_2 and O_2^- levels. LOX is a crucial enzyme that initiates membrane lipid metabolism through catalyzing polyunsaturated fatty acid oxidation, thereby producing hydrogen peroxide, which in turn induces lipid peroxidation in cell membranes [48]. Under stress, peroxidation of membrane lipids may result in damage to the cell membrane, decreased fluidity, enhanced permeability, and eventual leakage of extracellular fluid [49]. MDA levels are closely associated with cell membrane deterioration in fruits and vegetables, increased concentrations of MDA suggest a greater extent of damage to the structural integrity of these membranes [50]. Melatonin treatment notably decreased LOX activity and lowered MDA levels in fresh-cut yam tissues, indicating that the application of melatonin hinders the metabolism of membrane lipids. In the cells of fruits and vegetables, vacuoles serve as storage for phenolic compounds, whereas PPO is found in the cytoplasm. When there is damage to the cell membrane, phenolic compounds interact with PPO, leading to browning [51]. This suggests that the preservation of the cell membrane's integrity is essential for inhibiting browning. Melatonin treatment helps maintain cell membrane integrity by lowering ROS levels and retarding membrane lipid metabolism, thereby contributing to its anti-browning effect.

The phenylpropanoid pathway produces secondary metabolites such as flavonoids and phenolic compounds in plants. These compounds serve important functions in plant defense against various biotic and abiotic stresses [52]. The early steps of this pathway are catalyzed by PAL, C4H, and 4CL, which provide precursors for numerous downstream branches [53]. Intermediates such as coumaric acid, ferulic acid, and niacin are initially synthesized and then converted into coumarin esters, chlorogenic acid, and coenzyme A. This pathway ultimately leads to the production of secondary metabolites, including lignans, alkaloids, and flavonoids[54, 55] In this study, both PAL activity and expression were markedly lower in MT-treated samples than in the CK group. These results suggest that the PAL-catalyzed deamination of phenylalanine to trans-cinnamic acid was inhibited. Furthermore, reduced *4CL* expression lowered trans-cinnamic acid and p-coumaric acid-CoA production, thereby restricting precursors for phenolic biosynthesis. MT-treated samples showed significant downregulation of lignin- and phenolic biosynthesis-related genes (*COMT* and *CAD*), consistent with reduced phenolic content. These data suggest that MT treatment mitigated browning in fresh-cut yam by suppressing phenolic biosynthesis and decreasing browning-related enzyme activities, including PPO and POD. This conclusion was reinforced by decreases in phenolic content, enzyme activity, and browning-related gene expression. Our

findings align with Lin et al. [56], who reported that chlorine dioxide (ClO_2) fumigation can affect phenylpropanol.

Flavonoid biosynthesis represents a crucial phase in the phenylpropanoid metabolic pathway, generating over 6,000 compounds known for their antioxidant characteristics. These metabolites play an important role in reducing ROS and protecting plants from damage caused by oxidative stress [57]. However, certain flavonoids, such as 3-O-rutin, can cause yellowing and browning, and the re-synthesis and/or accumulation of these compounds on the cut surface may change the color of fresh-cut produce. Consequently, flavonoid build-up is regarded as another factor contributing to browning in fresh-cut products throughout storage. Changes in the composition and content of flavonoids markedly affect the color hue and browning susceptibility of apple flesh [58]. Moreover, studies have shown a close link between suppressed flavonoid biosynthesis and browning progression. For example, melatonin has been demonstrated to alleviate browning in fresh-cut lotus root during storage by reducing flavonoid synthesis [59]. Cinnamic acid has also been reported to alleviate browning in fresh-cut taro slices through inhibition of flavonoid biosynthesis and accumulation [60]. In the flavonoid biosynthetic pathway, CHS and CHI serve as critical rate-limiting enzymes [61,62], while C3'H and DFR mediate the production of dihydroflavonoids and anthocyanins [63].This study showed that genes encoding key enzymes in flavonoid biosynthesis (*CHS, CHI, C3'H*, and *DFR*) were downregulated in MT-treated samples. Such downregulation suggests that MT treatment may reduce flavonoid content by inhibiting flavonoid biosynthesis-related gene expression, thereby potentially contributing to the bright color retention of yam slices.

The link between starch and sucrose metabolism and browning has been well documented in numerous fruits and vegetables [64]. For instance, the internal browning observed in taro has been linked to an increase in sucrose metabolism. Research indicates that treatment with 6-BA can delay the breakdown of starch by lowering amylase levels, consequently postponing browning in lotus seeds [65]. Notably, abundant amyloplast accumulation induces ROS generation and promotes polyphenol biosynthesis, consequently leading to brown polymer formation [66]. Furthermore, sucrose stimulates its own synthesis and helps plants adapt to environmental stresses [67], potentially affecting browning triggered by stress in fruits and vegetables. Enzymes critical to the metabolism of starch and sucrose encompass *AMY, INV, SPS,* and *SUS* [68]. MT treatment in this study strongly reduced the expression of key starch–sucrose metabolism genes, such as *INV, AMY, bglB*, and *BAM*, while increasing sucrose content. These results imply that MT treatment may inhibit both the synthesis and breakdown of starch and sucrose throughout storage, which could help reduce browning. Similar links between starch–sucrose metabolism and browning have been reported in taro and lotus seeds [64, 65].

This study suggests that MT can directly inhibit enzymes associated with browning; however, the functions of key genes or enzymes have not yet been validated through methods such as

transient silencing or overexpression. Additionally, a distinction has not been made between MT's direct free radical scavenging and its signaling regulatory roles. Future studies should focus on the functional validation of key genes such as PAL, PPO, and POD, in conjunction with the detection of endogenous MT, MT receptors, and hormone signaling, to elucidate the mechanisms by which MT inhibits browning.

5. Conclusion

Melatonin treatment showed significant effectiveness in preventing enzymatic browning in fresh-cut *D. hemsleyi* in Weixi, while maintaining the quality of the slices over a storage period of four days following MT application. MT reduced browning by suppressing key phenol-oxidizing enzymes such as POD, PPO, and PAL. Transcriptomic and metabolomic data revealed that MT treatment lowered flavonoid and phenolic compound production and modulated the expression of starch–sucrose metabolism-related genes. These findings indicate that MT directly inhibits browning-associated enzymes and enhances antioxidant defense. MT treatment enhanced the quality and prolonged the shelf life of fresh-cut *D. hemsleyi* in Weixi; nevertheless, its potential applications in other crops vulnerable to browning under different storage conditions remain to be explored.

Acknowledgements

We appreciate all the people who have collaborated on this project.

Generative AI statement

The author(s) declare that no Generative AI was used in the creation of this manuscript.

Author contribution

S.Z.: Writing-review & editing, Writing-original draft, Validation, Visualization, Investigation, Data curation. L.Z.: Writing-review & editing, Validation, Supervision, Methodology, Investigation, Formal analysis, Data curation. M.Z.: Validation, Investigation, Formal analysis, Data curation. Z.L., X.M.: Validation, Methodology, Investigation, Data curation. G.Z.: Validation, Supervision, Methodology, Investigation, Formal analysis. W.Y., X.F.: Supervision, Resources, Project administration, Conceptualization. N.Z., Y.L., D.Z.: Writing-review & editing, Validation, Supervision, Resources, Project administration, Funding acquisition, Conceptualization. All authors read and approved the final manuscript.

Declaration of competing interest

The authors declare that they have no conflict of interest.

Funding

This study was financially supported by the Yunnan Provincial Major Science and

Technological Special Project (202402AE090021). The funders had no role in study design, data collection and analysis, decision to publish, or preparation of the manuscript.

Data availability

All data produced or examined throughout this research are contained within this published paper.

Declarations

Ethics approval and consent to participate

There are no ethical issues involved in this paper.

Consent for publication

Not applicable.

Competing interests

The authors declare no competing interests

References

1. Zhao C. Study on component distribution and bioactivity of medicinal plants from five allied genera of Paris and *Dioscorea* genus. [Doctoral dissertation, Tianjin University]. 2022. https://doi.org/10.27356/d.cnki.gtjdu.2022.004196
2. Liu MY, Zhang XC, Peng TT, Cao HT, Chen R, Liu PH, Yang F. Study on sugar content in underground tubers of three *Dioscorea* species from section Opsophyton. *J. Guizhou Univ. (Nat. Sci. Ed.)* 2024;41(1):54-58. https://doi.org/10.15958/j.cnki.gdxbzrb.2024.01.08
3. Wang YS, Shi ZJ, Zhang MXY, Cao CW, Kan H, Liu ZJ, Zhao GJ, Li F, Liu Y. Preparation and structural and functional properties of protein powder from *Dioscorea hemsleyi* in Weixi. *Food Ferment. Ind.* 2026;1-13. https://doi.org/10.13995/j.cnki.11-1802/ts.045626
4. Shi JZ, Du CY, Yang P, Feng SX, Cizhu LM, Peng HP, Li WL. Effects of different fertilization treatments on yield and quality of *Dioscorea hemsleyi* in Weixi.J. *Chin. Med. Mater*. 2024;47(5):1094-1099. https://doi.org/10.13863/j.issn1001-4454.2024.05.004
5. Liao XM, Xing YG, Fan XF, Qiu Y, Xu QL, Liu XC. Effect of composite edible coatings combined with modified atmosphere packaging on the storage quality and microbiological properties of fresh-cut pineapple. *Foods*. 2023;12(6):1344. https://doi.org/10.3390/foods12061344
6. Faisal M, Arshad N, Wang H, Li CC, Ma JJ, Kong XX, Luo HB, Yu LJ.. Recent advances in technologies for preserving fresh-cut fruits and vegetables. *Foods*. 2025; 14(16): 2769. https://doi. org/10.3390/foods14162769
7. Guo S, Ma Y, Wang YB, Zhao WT, Zheng YY, Wang P, Wang D, Zhao XY. Effects of storage temperature on bisdemethoxycurcumin formation in fresh-cut yam (*Dioscorea opposita*). *J. Food Compos. Anal.* 2021;103:104106. https://doi.org/10.1016/j.jfca.2021.104106
8. Cheng HY, Du HY, Zuo XX, Shen YG, Cai ZP, Wang J, Zhang W, Zhu LQ. Oxalic acid alleviates surface discoloration in fresh-cut yam by regulating enzymatic browning and bisdemethoxycurcumin synthesis. *LWT*. 2024;210:116836. https://doi.org/10.1016/j.lwt.2024.116836
9. Zhao PY, Li WD, Zhen CY, Wang K, Qin Z, Gao HY. Transcriptomic analysis of the effects of γ-aminobutyric acid treatment on browning and induced disease resistance in fresh-cut apples. *Postharvest Biol. Technolo*. 2021;181:111686. https://doi.org/10.1016/j.postharvbio.2021.111686
10. Wang WY, Hu JX, Chen WN, Li X, Bi JF. Metabolomic analysis reveals the browning related enzymes and metabolic pattern differences in apples of different storage periods. *Food Chem. X*. 2025;29:102681. https://doi.org/10.1016/j.fochx.2025.102681
11. Ali S, Khan AS, Anjum MA, Nawaz A, Naz S, Ejaz S, Hussain S. Effect of postharvest oxalic acid application on enzymatic browning and quality of lotus (*Nelumbo nucifera*

Gaertn.) root slices. *Food Chem*. 2020;312:126051. https://doi.org/10.1016/j.foodchem.2019.126051

12. Guo S, Wang D, Ma Y, Zhang Y, Zhao XY. Combination of RNA-Seq transcriptomics and iTRAQ proteomics reveal the mechanism involved in fresh-cut yam yellowing. *Sci Rep*. 2021; 11(1):7755. https://doi. org/10.1038/s41598-021-87423-4
13. Yepes-Betancur DP, Zapata-Vahos IC, Henao-Rojas JC, Martinez-Saldarriaga J, Márquez-Cardozo CJ, Cadena-Chamorro EM. Inhibitory effect of fermented avocado seed extract (Persea americana Mill. cv. Hass) on polyphenol oxidase and its application as anti-browning agent in avocado, apple, and banana pulps. *Heliyon*. 2025;11(4):https://doi.org/10.1016/j.heliyon.2025.e42588
14. Zhang GJ, Gu LB, Lu ZF, Yuan C, Sun YH. Browning control of fresh-cut Chinese yam by edible coatings enriched with an inclusion complex containing star anise essential oil. *RSC Adv*. 2019;9(9):5002-5008. https://doi.org/10.1039/c8ra08295b
15. Guo S, Zhao XY, Ma Y, Zhang Y, Wang D. Ethanol treatment suppresses the yellowing of fresh-cut yam by repressing the phenylpropanoid pathway and bisdemethoxycurcumin biosynthesis. *Postharvest Biolo. Technolo.* 2023*;*181:111642. https://doi.org/10.1016/j.postharvbio.2021.111642
16. Zhao XY, Guo S, Ma Y, Zhao WT, Wang P, Zhao S, Wang D. Ascorbic acid prevents yellowing of fresh-cut yam by regulating pigment biosynthesis and energy metabolism. *Food Res. Int*. 2024;157:111424. https://doi.org/10.1016/j.foodres.2022.111424
17. Zhao XY, Guo S, Zhao WT, Wang P, Zhao S, Xu YJ, Wang D. Regulation mechanism of sodium citrate on fresh-cut yam yellowing. *Postharvest Biol. Technol*. 2022;191:111965. https://doi.org/10.1016/j.postharvbio.2022.111965
18. Gao J, Hu XM, Luo FY, Tang YM, Luo JH, Yang YW. Changes in bacterial community characteristics on surface of fresh-cut yams during cold storage after ethanol combined ascorbic acid washing. *LWT*. 2024; 201, 116250. https://doi.org/10.1016/j.lwt.2024.116250
19. Pang X, Lin ZX, Wang MN, Liang HF, Zhao YQ, Li Y, Yan BJ, He YY, Wu XX, Wang Q, Feng BH. Mechanisms underlying the effect of high-temperature curing treatments on the browning response of fresh-cut yams. *Food Chem*. 2025;476:143317. https://doi.org/10.1016/j.foodchem.2025.143317
20. Tang Q, Li CY, Ge YH, Li X, Cheng Y, Hou JB, Li JR. Exogenous application of melatonin maintains storage quality of jujubes by enhancing anti-oxidative ability and suppressing the activity of cell wall-degrading enzymes. *LWT*. 2020;127:109431. https://doi.org/10.1016/j.lwt.2020.109431
21. Ahamad S, Asrey R, Singh AK, Sethi S, Joshi A, Vinod BR, Meena NK, Menaka M, Choupdar GK. Melatonin treatment enhances bioactive compound retention, antioxidant activity and shelf-life of bell pepper (*Capsicum annuum* L.) during cold storage. *Int. J. Food Sci. Technol*. 2023;59(10):7918-7931. https://doi.org/10.1111/ijfs.17154

22. Kanwar MK, Yu JQ, Zhou J. Phytomelatonin: recent advances and future prospects. *J. Pineal Res*. 2018;65(4):12526. https://doi. org/10.1111/jpi.12526
23. Huang TY, Kou XH, Qiao LX, Li JK, Luo DL, Wang XF, Cao S. Maintaining quality of postharvest green pepper fruit using melatonin by regulating membrane lipid metabolism and enhancing antioxidant capacity. *Food Chem*. 2023;460:140671. https://doi. org/10.1016/j.foodchem.2024.140671
24. Aghdam MS, Fard JR. Melatonin treatment attenuates postharvest decay and maintains nutritional quality of strawberry fruits (Fragaria× anannasa cv. Selva) by enhancing GABA shunt activity. *Food Chem*. 2017;221:1650-1657. https://doi. org/10.1016/j.foodchem.2016.10.123
25. Dan YH, Zhang S, Zhong H, Yi HC, Sainz MB. Novel compounds that enhance Agrobacterium-mediated plant transformation by mitigating oxidative stress. *Plant cell Rep*. 2015;34(2):291-309. https://doi. org/10.1007/s00299-014-1707-3
26. Wu CH, Cao SF, Xie KQ, Chi ZY, Wang J, Wang HF, Wei YY, Shao XF, Zhang CD, Xu F, Gao HY. Melatonin delays yellowing of broccoli during storage by regulating chlorophyll catabolism and maintaining chloroplast ultrastructure. *Postharvest Biol. Technol*. 2021;172:111378. https://doi.org/10.1016/j.postharvbio.2020.111378
27. Sharafi Y, Jannatizadeh A, Fard JR, Aghdam MS. Melatonin treatment delays senescence and improves antioxidant potential of sweet cherry fruits during cold storage. *Sci Hortic*. 2021;288:110304. https://doi.org/10.1016/j.scienta.2021.110304
28. Zheng HH, Liu W, Liu S, Liu CH, Zheng L. Effects of melatonin treatment on the enzymatic browning and nutritional quality of fresh-cut pear fruit. *Food Chem*. 2019;299: 125116. https://doi.org/10.1016/j.foodchem.2019.125116
29. Min T, Xie J, Zheng ML, Yi Y, Hou WF, Wang LM, Ai YW, Wang HX. The effect of different temperatures on browning incidence and phenol compound metabolism in fresh-cut lotus (*Nelumbo nucifera* G.) root. *Postharvest Biol. Technol*. 2017;123:69-76. https://doi.org/10.1016/j.postharvbio.2016.08.011
30. Wu XP, Li QY, Yi Y, Wang LM, Hou WF, Ai YW, Wang HX, Min T. Cinnamaldehyde affects the storage quality of freshly cut water chestnuts through the regulation of reactive oxygen species and the AsA-GSH cycle. *Scientia Horticulturae*. 2024;332:113199. https://doi.org/10.1016/j.scienta.2024.113199
31. Mishra BB, Gautam S, Sharma A. Purification and characterisation of polyphenol oxidase (PPO) from eggplant (Solanum melongena). *Food Chem*. 2012;134(4):1855-1861. https://doi.org/10.1016/j.foodchem.2012.03.098
32. Chen LF, Meng Y, Jiang DW, Yang FR, Zhou YW. Physio-biochemical responses of three Aquilegia species seedlings to salt stress. *Agronomy*. 2022;12(11):2841. https://doi.org/10.3390/agronomy12112841
33. Wei HJ, Wang JJ, Wang Q, He WY, Liao SK, Huang JH, Hu WT, Tang M, Chen H. Role of melatonin in enhancing arbuscular mycorrhizal symbiosis and mitigating cold stress in

perennial ryegrass (*Lolium perenne* L.). *Front. Microbiol*. 2023;14:1123632. https://doi.org/10.3389/fmicb.2023.1123632

34. Pang X, Lin ZX, Liang HF, Shi JY, Yuan SZ, Yue XZ, Xu XD, Zhao YQ, Wei ZF, Zuo JH, Sui Y, Feng BH, Wang Q. Combined physiological, biochemical, and multi-omic analyses provide insight into the cause of differential browning in early and late harvested fresh-cut yams. *Postharvest Biol. Technol*. 2025;221:113324. https://doi.org/10.1016/j.postharvbio.2024.113324
35. Kuagny RBM, Saha BUF, Achu MBL, Kansci G, Medoua GN, Fokou E. Polyphenol and flavonoid contents, antioxidant activities and glycaemic index of *Dioscorea* spp and *Coleus* esculentus from Cameroon. *Food Chem. Adv*. 2023;3:100500. https://doi.org/10.1016/j.focha.2023.100500
36. Xing LN, Zhang YF, Xing YP, Ge MR, Miao HQ, Huo XW. Reference genes selection and validation in yam by real-time quantitative polymerase chain reaction. *Sci Rep*. 2025;15(1):19947. https://doi.org/10.1038/s41598-025-92244-w
37. Xiao YH, Xie J, Wu CS, He JM, Wang B. Effects of melatonin treatment on browning alleviation of fresh-cut foods. *J. Food Biochem*. 2021;45(9):13798. https://doi.org/10.1111/jfbc.13798
38. Gao H, Zhang ZK, Chai HK, Cheng N, Yang Y, Wang DN, Yang T, Cao W. Melatonin treatment delays postharvest senescence and regulates reactive oxygen species metabolism in peach fruit. *Postharvest Biol. Technol.* 2016;118:103-110. https://doi.org/10.1016/j.postharvbio.2016.03.006
39. Min T, Lu KY, Chen JH, Niu LF, Lin Q, Yi Y, Hou WF, Ai YW, Wang HX. Biochemical mechanism of fresh-cut lotus (*Nelumbo nucifera* Gaertn.) root with exogenous melatonin treatment by multiomics analysis. *Foods*. 2022;12(1):44. https://doi.org/10.3390/foods12010044
40. Ma XY, Wang H, Wang XJ, Li XY, Li H, Wang DQ, Yang Y. Melatonin activates phenylpropanoid metabolism and antioxidant defense to preserve quality of fresh-cut potatoes during cold storage. *Foods*. 2026;15(7):1234. https://doi.org/10.3390/foods15071234
41. Yuan X, Zhan ZX, Lin W, Zhang C, Wang B. The membrane may be a key factor influencing browning: a mini review on browning mechanisms of fresh-cut fruit and vegetables from a multi-omics perspective. *Front. Nutr*. 2025;12:1534594. https://doi.org/10.3389/fnut.2025.1534594
42. Rasane P, Singh J, Kaur S, Bakshi M, Gunjal M, Kaur J, Sharma KP, Sachan S, Singh A, Bhadariya V, Mahato DK. Strategic advances in the management of browning in fruits and vegetables. *Food and Bioprocess Technol*. 2024;17(2):325-350. https://doi.org/10.1007/s11947-023-03128-8
43. Wang C, Dai LP, Bai XR, Zhang S, Dai PQ, Zhao BL, Zhao FY, Hu DG. Nicotinamide delays browning in fresh-cut apples through reducing Chlorogenic acid and inhibiting

PPO activity. *Food Chem*. 2025;146738. https://doi.org/10.1016/j.foodchem.2025.146738

44. Guan QH, Li WH, Dai M, Qiao J, Wu B, Zhang Z, Shi JY, Song ZY. Key factors uncovered by transcriptomic analysis in the regulation of glutamic acid repressing the browning of fresh-cut potatoes. *Postharvest Biol. Technol*. 2025;219:113242. https://doi.org/10.1016/j.postharvbio.2024.113242
45. Pan YF, Chen L, Pang LL, Chen XT, Jia XY, Li XH. Ultrasound treatment inhibits browning and improves antioxidant capacity of fresh-cut sweet potato during cold storage. *RSC Adv*. 2020;10(16):9193-9202. https://doi.org/10.1039/c9ra06418d
46. Chouaibi Y, Ben Romdhane W, Wiszniewska A, Baazaoui N, Bouteraa MT, Gamas N, Jrad O, Kačániová M, Kluz MI, Ben Hsouna A, Ben Saad R. TdNF-YA2A-1 transcription factor confers salt and osmotic stress tolerance in tobacco through regulation of the antioxidant defense system. *Plant Signal. Behav.* 2026;21(1):2608488. https://doi. org/10.1080/15592324.2025.2608488
47. Wei LY, Liu CH, Wang JJ, Younas S, Zheng HH, Zheng L. Melatonin immersion affects the quality of fresh-cut broccoli (*Brassica oleracea* L.) during cold storage: Focus on the antioxidant system. *J. Food Process. Preserv.* 2020;44(9):14691. https://doi.org/10.1111/jfpp.14691
48. Wang D, Li D, Xu YQ, Li L, Belwal T, Zhang XC, Luo ZS. Elevated CO2 alleviates browning development by modulating metabolisms of membrane lipids, proline, and GABA in fresh-cut Asian pear fruit. *Sci Hortic*, 281, 109932. https://doi.org/10.1016/j.scienta.2021.109932
49. Ali S, Khan AS, Malik AU. Postharvest L-cysteine application delayed pericarp browning, suppressed lipid peroxidation and maintained antioxidative activities of litchi fruit. *Postharvest Biol. Technol*. 2016;121:135-142. https://doi.org/10.1016/j.postharvbio.2016.07.015
50. Gao H, Kang LN, Liu Q, Cheng N, Wang BN, Cao W. Effect of 24-epibrassinolide treatment on the metabolism of eggplant fruits in relation to development of pulp browning under chilling stress. *J. Food Sci. Technol.* 2015;52(6):3394-3401. https://doi.org/10.1007/s13197-014-1402-y
51. Murata M.. Food chemistry and biochemistry of enzymatic browning. *Food Sci. Technol. Res*. 2022;28(1):1-12. https://doi.org/10.3136/fstr.FSTR-D-21-00130
52. Castro-Cegrí A, Sierra S, Hidalgo-Santiago L, Esteban-Muñoz A, Jamilena M, Garrido D, Palma F. Postharvest treatment with abscisic acid alleviates chilling injury in zucchini fruit by regulating phenolic metabolism and non-enzymatic antioxidant system. *Antioxidants*. 2023;12(1):211. https://doi. org/10.3390/antiox12010211
53. Liu MY, Zhang XC, Peng TT, Cao HT, Chen R, Liu PH, Yang F. Mechanisms of the response of apple fruit to postharvest compression damage analyzed by integrated transcriptome and metabolome. *Food Chem. X.* 2023;20:100972.

https://doi.org/10.1016/j.fochx.2023.100972
54. Bhushan B, Pal A, Narwal R, Meena VS, Sharma PC, Singh J. Combinatorial approaches for controlling pericarp browning in Litchi (Litchi chinensis) fruit. *J. Food Sci. Technol.* 2015;52(9):5418-5426. https://doi. org/10.1007/s13197-015-1712-8
55. Liu WX, Feng Y, Yu SH, Fan ZQ, Li XL, Li JY, Yin HF. The flavonoid biosynthesis network in plants. *Int J Mol Sci*. 2021;22(23):12824. https://doi.org/10.3390/ijms222312824
56. Lin ZX, Yao RC, Pang X, Liang HF, Li Y, Wu XX, Yan X, Yuan SZ, Xu XD, Jiang AL, Feng BH, Yue XZ, Wang Q. ClO2 fumigation of yam tubers prior to storage inhibits enzymatic Browning in fresh-cut yams: impact of ClO2 on phenylpropanoid metabolism and membrane integrity. *Food Chem*. 2026;501:147567. https://doi. org/10.1016/j.foodchem.2025.147567
57. Nabavi SM, Šamec D, Tomczyk M, Milella L, Russo D, Habtemariam S, Suntar I, Rastrelli L, Daglia M, Xiao J, Giampieri F, Battino M, Sobarzo-Sanchez E, Nabavi SF, Yousefi B, Jeandet P, Xu S, Shirooie S. Flavonoid biosynthetic pathways in plants: Versatile targets for metabolic engineering. *Biotechnol Adv*. 2020;38:107316. https://doi.org/10.1016/j.biotechadv.2018.11.005
58. Fang T, Chen J, Lin Q, Zhong YG, Duan YQ, Bi JF. Phenolic profiling reveals the metabolite basis of flesh colour and fresh-cut browning in apple fruit. *Int J Food Sci Technol*. 2022;57(4):2257-2266. https://doi. org/10.1111/ijfs.15575
59. Zhang C, Xin Y, Wang ZW, Qin LL, Cao LY, Li HF, Ma XT, Yin JY, Zhao ZX, Liu PJ, Tang JW, Dong C. Melatonin-induced myeloblastosis viral oncogene homologs alleviate fresh-cut lotus root browning during storage by attenuating flavonoid biosynthesis and reactive oxygen species. *J Sci Food Agric*. 2023;103(11):5452-5461. https://doi.org/10.1002/jsfa.12619
60. Xiao YH, Zhang JL, Jiang YY, Yuan Y, Xie J, He JM, Wang B. Cinnamic acid treatment reduces the surface browning of fresh-cut taro. *Sci Hortic*. 2022;291:110613. https://doi.org/10.1016/j.scienta.2021.110613
61. Deng X, Bashandy H, Ainasoja M, Kontturi J, Pietiäinen M, Laitinen RAE, Albert VA, Valkonen JPT, Elomaa P, Teeri TH. Functional diversification of duplicated chalcone synthase genes in anthocyanin biosynthesis of Gerbera hybrida. *New Phytol*. 2014;201(4):1469-1483. https://doi. org/10.1111/nph.12610
62. Liu XH, Zhang AD, Shang J, Zhu ZW, Li Y, Wu XX, Zha DS. Study on browning mechanism of fresh-cut eggplant (Solanum melongena L.) based on metabolomics, enzymatic assays and gene expression. *Sci Rep*. 2021;11:6937. https://doi.org/10.1038/s41598-021-86311-1
63. LaFountain AM, Yuan YW. Repressors of anthocyanin biosynthesis. New Phytol. 2021;231(3):933-949. https://doi. org/10.1111/nph.17397
64. Zhu J, Ge TY, Nian LY, Liu Y, Miao YY, Wang SL, Cao CJ. Low frequency polarized

electric field inhibits enzymatic browning in fresh-cut taro via dual regulation of carbohydrate metabolism and ROS scavenging systems. *Postharvest Biol Technol*. 2025;230:113808.. https://doi.org/10.1016/j.postharvbio.2025.113808

65. Luo SF, Hu HL, Zhang LG, Zhou HS, Li PX. Sugars in postharvest lotus seeds were modified by 6-benzylaminopurine treatment through altering related enzymes involved in starch-sucrose metabolism. *Sci Hortic.* 2017;221:73-82. https://doi.org/10.1016/j.scienta.2017.03.044
66. Fukuoka N, Miyata M, Hamada T, Takeshita E. Occurrence of internal browning in tuberous roots of sweetpotato and its related starch biosynthesis. *Plant Physiol Biochem*. 2019;135:233-241. https://doi. org/10.1016/j.plaphy.2018.12.007
67. Zhao J, Quan PK, Liu HK, Li L, Qi SY, Zhang MS, Zhang B, Li H, Zhao YR, Ma BQ, Han MY, Zhang HH, Xing LB. Transcriptomic and metabolic analyses provide new insights into the apple fruit quality decline during long-term cold storage. *J Agric Food Chem*. 2020;68(16):4699-4716. https://doi.org/10.1021/acs.jafc.9b07107
68. Zhang Q, Tang FX, Cai WC, Peng B, Ning M, Shan CH, Yang XQ. Chitosan treatment reduces softening and chilling injury in cold-stored Hami melon by regulating starch and sucrose metabolism. *Front Plant Sci*. 2022;13:1096017. https://doi.org/10.3389/fpls.2022.1096017

Supplementary Files

This is a list of supplementary files associated with this preprint. Click to download.

- Graphicalabstract.docx
- SupplementaryFigure.docx
- SupplementaryTable.docx